A&A 371, 1065–1077 (2001)
DOI: 10.1051/0004-6361:20010400

Astronomy & Astrophysics

Spectra of carbon-rich asymptotic giant branch stars between 0.5 and 2.5 μm: Theory meets observation

R. Loidl[1], A. Lançon[2], and U. G. Jørgensen[3]

[1] Institut für Astronomie der Universität Wien, Türkenschanzstraße 17, 1180 Wien, Austria
[2] Observatoire de Strasbourg, UMR 7550, 11 rue de l'Université, 67000 Strasbourg, France
[3] Niels Bohr Institute, Astronomical Observatory, Juliane Maries Vej 30, 2100 Copenhagen, Denmark

Received 21 July 2000 / Accepted 13 March 2001

Abstract. We present a hydrostatic analysis of five carbon rich stars, BH Cru, T Cae, S Cen, RU Pup and Y Hya in the wavelength range between 0.5 and 2.5 μm. All except BH Cru, which is a Mira star, show only modest variability. We identify the absorption features of the molecules CO, CN and C_2. The overall energy distribution, which is very sensitive to the effective temperature in the investigated wavelength range, as well as the bands of these molecules put strict limits on the possible values of effective temperature and C/O. We show that our model atmospheres and corresponding synthetic spectra are able to reproduce the observed spectra quite accurately from about 0.7 to 2.5 μm. The discrepancies are mainly due to uncertainties in the molecular input data. We discuss briefly why the variations of the molecular features are small and why dynamic phenomena do not play a very important role in this wavelength range. We identify colour indices based on commonly available filters and potentially suitable for the empirical determination of fundamental parameters of carbon stars.

Key words. stars: AGB and post-AGB – stars: atmospheres – stars: variables – stars: carbon – radiative transfer

1. Introduction

Theoretical stellar spectra in satisfactory agreement with observations have become available over the last decades for stars located almost anywhere in the HR diagram, providing us with tools to investigate fundamental stellar properties by spectrophotometric means (e.g. Bessell et al. 1998). The coolest stars have been known as one of the challenging exceptions. Since infrared (IR) observational technology became available, considerably increasing our knowledge about the empirical properties of cool stars, a huge effort has gone into the obtention of fundamental molecular input data and numerical methods to deal with the radiative transfer when millions of molecular lines are relevant. The results have shown rapid progress, as illustrated by improving fits to empirical data (e.g. Goebel et al. 1980; Lambert et al. 1986; Jørgensen 1989; Jørgensen et al. 2000 for carbon stars; Tsuji et al. 1997 for cool luminous oxygen-rich stars; Leggett et al. 2000 for M type dwarfs).

In this paper we focus on five cool carbon rich giant stars which are assumed to be the product of carbon dredge-up on the asymptotic giant branch (AGB). Most upper AGB stars pulsate with periods of about 100 to 1000 days; in their atmospheres, the density-temperature structure is dependent on dynamical phenomena, such as shock waves and stellar winds. In addition, the formation of molecules and dust grains plays an important role. Since most of the model spectra discussed here are based on hydrostatic model atmospheres, we have restricted ourselves to comparisons to observations of moderately variable (mostly semi-regular) stars.

Recently, Jørgensen et al. (2000) presented fits to the spectra of three moderately variable carbon stars in the wavelength range between 2.5 and 20 μm covered by the Infrared Space Observatory (ISO). They showed that the spectra of AGB stars with insignificant pulsation and which are not surrounded by a lot of hot dust can be fitted quite well till about 10 μm. Our synthetic spectra are based on the same model structures and molecular input data as theirs. The present paper considerably extends the model validation towards short wavelengths: for the first time, we present a comparison with spectra that range from 0.5 to 2.5 μm, taken in joint observations with an optical and a near-IR telescope and thus avoiding potential pulsation phase or cycle mismatch. As AGB stars emit the bulk of their luminosity in the near-IR, it was essential to check the models also in this wavelength region, and by stretching the observations to 2.5 μm it was possible to fully complement the ISO SWS spectral range.

Send offprint requests to: R. Loidl,
e-mail: loidl@astro.univie.ac.at

The variations of the intensities of the molecular features of carbon stars in the optical and near infrared range are smaller than in the mid infrared region. In Sect. 3 we discuss why the inclusion of dynamic phenomena is less important in this wavelength range than further in the infrared. This fact, combined with the selection of low amplitude variables, makes the use of hydrostatic atmospheres acceptable for studies of the effective temperature, the C/O abundance ratio and the isotopic ratio $^{12}C/^{13}C$. The spectra, on the other hand, are little sensitive to atmospheric extension or surface gravity. Model inputs and the influence of stellar parameters are described in Sect. 4.

In Sects. 5 and 6 the comparison between observed and model spectra is presented and remaining discrepancies are discussed. Using passbands of commonly available filters, we discuss colour indices that may become useful direct indicators of fundamental stellar properties in Sect. 7. Section 8 summarises the results.

2. Observations

The near-IR spectra were obtained on the Australian National University 2.3 m Telescope at Siding Spring Observatory, using the cross-dispersed grism mode of the Cryogenic Array Spectrometer and Imager CASPIR. For each of the IJ, JH and HK grisms, five orders are imaged onto the CASPIR array. The spectra were acquired through the $1'' \times 15''$ slit providing a resolving power of approximately 1100. Low resolution optical spectra were acquired using the so-called Reynolds Spectrograph at the 1.88 m Telescope on Mount Stromlo. Details about the data reduction can be found in Lançon & Wood (2000). Here, we only briefly recall the properties of the resulting spectra.

The pixel-to-pixel noise in the spectra is due to photon and read-out noise, to residual telluric absorption features, and in the optical to changing seeing-determined spectral resolution and calibration. The signal-to-noise ratio per resolved element typically has values around 50 in clear atmospheric windows ($1\,\sigma$ noise). It drops strongly in regions of strong telluric CO_2 or H_2O absorption.

The uncertainties on the energy distribution and colours result from the combined effects of instrumental changes, of the focusing and positioning of the stellar image on the slit, of the choice of a model for the intrinsic spectrum of the spectrophotometric reference stars, and of telluric absorption that reaches into the overlap region between the optical and near-IR data. An uncertainty of 0.15 mag affects colours that combine optical and near-IR fluxes. The uncertainty on purely near-IR colours increases with the separation between the central wavelengths of the combined filters; in most cases, it remains below 0.1 mag for a separation of 1 μm.

Table 1 lists the observed carbon stars used in this paper. All spectra are plotted in Lançon & Wood (2000). Here, we will not discuss the extremely cool large amplitude carbon rich Mira R Lep, for which circumstellar dust is likely to already play a significant role.

Table 1. Main properties of observed carbon stars

Name	variability type	δV	Period [1] (days)	Spectral type
Y Hya	SRb	3.7 [2]	302.8	C5,4 (N3P)
BH Cru	M	2.8	421.0	SC4,5/8e
S Cen	SR	1.5	65	C
T Cae	SR	1.8	156	C6,4 (N4)
RU Pup	SRb	1.9	425	C5,4 (N3)

[1] Periods as given in the GCVS of Kholopov et al. (1988).
[2] Significantly overestimated according to AAVSO/AFOEV data.

3. Variations

Except for S Cen at least 3 observations (up to 6) exist for each star (see Table 2). Only the Mira variable BH Cru shows remarkable variations in the spectra. The phase coverage for Y Hya and RU Pup is good: we can expect to have sampled the full amplitude of the variations. For T Cae at least half of the amplitude is sampled. Table 2 lists the date of observation and the corresponding phases of the observed carbon stars. Except for BH Cru phase 0.00 was assigned to the first observation of each star and the following phases were then calculated starting from this phase. For BH Cru it was possible to assign an absolute phase with the help of AAVSO data (Mattei 1999), our first spectrum was taken close to maximum light (phase 0.03). The period of BH Cru changed considerably during the last years (Bedding et al. 2000), around the time our spectra were taken it had increased to about 520 days.

Figure 1 shows the flux ratio of spectra obtained at two phases. The variations of RU Pup are representative for the other semi-regular variables too. All the C-type stars in our sample are classified as SRb or SR, indicating that they show relatively small variations in the luminosity. The shaded areas in the figure are spectral regions where the Earth's atmosphere prevents reliable observations. For RU Pup it is seen that except for these regions, the flux ratio is almost constant from 0.5 to 2.5 μm, illustrating that the spectra change very little with phase for the four semi-regular C-type stars. The flux ratio value of about 0.4 is caused by the fact that is was not possible to recover absolute flux values for RU Pup.

The small spectral variations with phase for the C-type stars between 0.5 and 2.5 μm are in strong contrast to the spectra of oxygen rich Long Period Variables (LPVs) which show prominent variations over a cycle. In oxygen rich stars the main contributing molecules are CO, TiO and H_2O. Both TiO and H_2O are temperature sensitive molecules. They are formed approximately between 2500 and 3500 K and between 2000 and 3000 K, respectively. In the atmospheric region corresponding to these temperatures dynamic effects like shocks and a levitation of the atmosphere compared to hydrostatic models play an important role (see e.g. Höfner et al. 1998). In carbon rich stars, the main contributing molecules between 0.5 and

Table 2. Dates of observation and corresponding phases of the observed carbon stars

name	period	date	phase
Y Hya	303	18 Jun. 1995	0.00
		8 Dec. 1995	0.57
		29 Jan. 1996	0.74
		3 Mar. 1996	0.85
		26 May 1996	1.13
		8 Jul. 1996	1.27
T Cae	156	8 Dec. 1995	0.00
		29 Jan. 1996	0.33
		3 Mar. 1996	0.55
RU Pup	425	4 Jun. 1995	0.00
		8 Dec. 1995	0.44
		29 Jan. 1996	0.56
		3 Mar. 1996	0.64
		26 May 1996	0.84
BH Cru	520	29 Jan. 1996	0.03
		26 May 1996	0.26
		8 Jul. 1996	0.34
S Cen	65	29 Jan. 1996	

2.5 μm are CO, CN and C_2. These molecules are formed deeper in the atmosphere at higher temperatures than the ones contributing in the oxygen rich case, mainly approximately between 3000 and 5000 K. In this region the influence of dynamics is much smaller. Therefore the variation of the molecular bands is much smaller over a cycle for carbon rich stars than for oxygen rich ones. This fact enables us to fit our observations of carbon-rich variable stars reasonably well with synthetic spectra based on hydrostatic model atmospheres which is not the case for oxygen-rich stars (e.g. Alvarez & Plez 1998; Schultheis 1998).

The only Mira star in the sample (BH Cru) is an SC star, and in this case we see a much stronger variation in band intensities (Fig. 1) and effective temperature than for the four semi-regulars.

4. Hydrostatic models and spectral synthesis

The model atmospheres are computed by use of an updated version of the original MARCS code (Gustafsson et al. 1975). Some of the improvements in the present version have been described by Jørgensen et al. (1992), Helling et al. (1996), and Jørgensen (1997). We treat the energy balance in the opacity sampling scheme, and have adopted approximately 10 000 frequency points for the radiative transfer computation. We include the molecules CO (from Goorvitch & Chackerian 1994), CN (from Jørgensen & Larsson 1990), C_2 (from Querci et al. 1974), CH (from Jørgensen et al. 1996), HCN, C_2H_2, and C_3 (as described in Jørgensen 1997) in the opacity, together with continuum sources as described in Gustafsson et al. (1975). The CN opacities have been improved compared to Jørgensen & Larsson (1990), by including also the violet system, and the C_2 opacities have been modified somewhat in the infrared spectral range as described in the following.

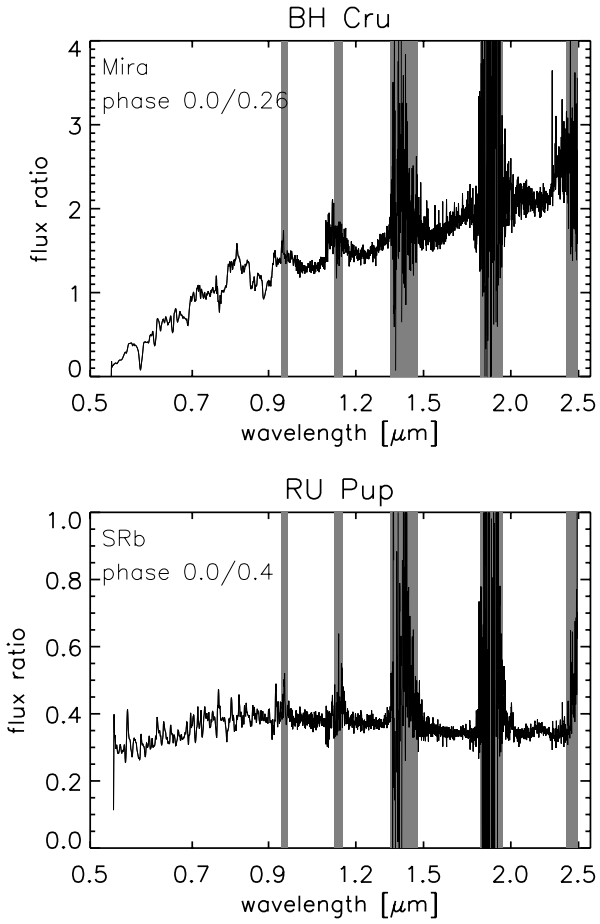

Fig. 1. Flux ratio of two different phases of the Mira star BH Cru (top) and the semi-regular variable RU Pup (bottom; note that most of the noise in the optical range is due to spectral resolution/calibration mismatch)

Several intense bands of C_2 are visible in our observed spectra, and C_2 bands have been used by several authors in the classification of carbon stars. Three line lists are described in the literature. One is due to Querci et al. (1971). Another is due to R. F. Kurucz (referred to in several of Kurucz' papers and reviews, for example in Kurucz 1994). The third and newest list is the compilation by Goorvitch (1990).

The lists due to Querci and due to Kurucz are both quite complete in their wavelength coverage, and they agree well with one another in the visual region. Goorvitch's compilation is limited to the two Ballik-Ramsay $b^3\Sigma_g^- - a^3\Pi_u$, $\Delta v = -1$ and -2 transitions centred at 2.5 μm and 4.3 μm. This list seems to be the most complete in the spectral region it covers, but its integrated band strength is approximately a factor 20 smaller than the corresponding one derived from Querci's list in the same region. The result of Kurucz is somewhere in between the two other lists in this region, although closer to the results of Goorvitch than to the results of Querci.

In the analysis we present here we have attempted to take advantage of the complete wavelength coverage of Querci's list together with the possible higher accuracy

of Goorvitch's more recent results, by scaling Querci's data to Goorvitch's data in the infrared spectral region. In praxis Querci's gf-values were divided by 10 long-ward of 1.5 μm where basically all lines belong to the Ballik-Ramsay system. Short-ward of 1.15 μm the list is dominated by the Phillips system, for which the two existing lists are in good mutual agreement. The region from 1.15 μm to 1.5 μm is dominated by a combination of lines from the Phillips $\Delta v = 0$ and $\Delta v = -1$ and the Ballik-Ramsay $\Delta v = +2$ and $\Delta v = +1$ systems. In order to ensure continuity in the scaling and at the same time simulate the increasing relative importance of the Ballik-Ramsay system at longer wavelengths, all gf-values (no line identification exist on Querci's list) here were divided with a number which increased linearly from 1 at 1.15 μm to 10 at 1.5 μm. We believe the resulting line list is a better representation of the real absorption coefficient than the unscaled Querci-list. We are presently working on a synthetic spectrum modelling of the few identifiable Ballik-Ramsay ($\Delta v = 0$) lines in the solar spectrum (Sauval & Jørgensen 2001, in preparation), which hopefully will contribute to confine the problem further and result in a better C_2 line list for future studies.

The model atmosphere computations assume hydrostatic equilibrium and are done in plane parallel geometry. We performed test computations in spherical geometry, but the effects of sphericity were found to be modest for stars in the parameter space discussed in the present paper and it did not alter our results derived from plane-parallel models. Effects of sphericity on carbon stars were analysed in detail by Jørgensen et al. (1992). The properties of a model atmosphere are determined by the effective temperature $T_{\rm eff}$, the surface gravity $\log(g)$, the mass M (although only for spherical geometry) and the heavy element composition, in particular the abundance ratio C/O and the isotopic ratio $^{12}C/^{13}C$.

Based on the model structure we computed the synthetic spectra by evaluating (1) the chemical abundances assuming equilibrium chemistry, (2) the continuum absorption using routines from the MARCS code (Gustafsson et al. 1975) and (3) the molecular opacities as a function of wavelength using the opacity sampling (OS) method. The chemistry routines are those of Tsuji (1973), with updated data as described in Helling et al. (1996) except for data for C_3 which are from Irwin (1981). For the computation of the synthetic spectra we use a larger frequency set of our opacity samplings than the one used for the model construction. The spectral sampling density corresponds to approximately 30 000 frequencies through the interval from 0.5 to 2.5 μm, or a resolution of approximately 20 000. Due to the statistical character of the opacity sampling technique, it is necessary to average the OS spectrum over a number of frequencies before it can be compared to an observed spectrum. The observed spectra have a resolution of approximately 1000 in the near-IR, and the corresponding synthetic OS spectra have therefore been averaged in order to obtain the same resolution, which means that each final computed spectral point is an average over

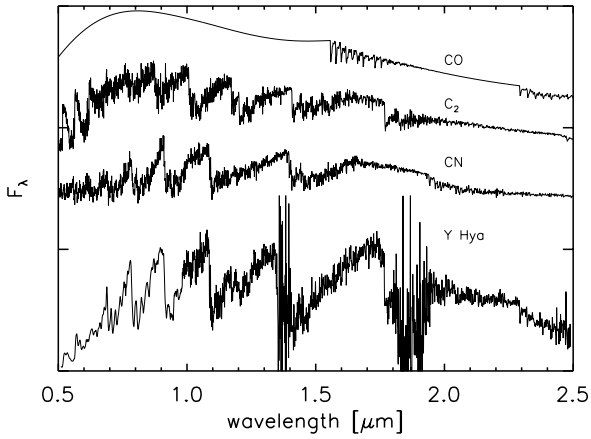

Fig. 2. Observed spectrum of Y Hya (bottom) and the contributions of the molecules CO, C_2 and CN to a synthetic spectrum with $T_{\rm eff} = 3000$ K, $\log(g) = 0.0$, C/O = 1.4, $v_{\rm mic} = 3\,{\rm km\,s^{-1}}$ and $^{12}C/^{13}C = 89$

20 OS radiative transfer calculations. This results in a computed spectrum which resembles well a "true" synthetic spectrum, i.e. one computed directly from the line lists and with "infinite" spectral resolution in the radiative transfer solution. When the line density is large there is a tendency for the OS spectrum technique to overestimate the absorption a bit, and vice versa when the line density is small. The higher the frequency density in the sampling the more accurate is the final spectrum, and experience has shown that an over-sampling with a factor of 20 gives a very realistic spectrum for this kind of stars.

While the plotted synthetic spectra have a resolution of 1000 between 0.987 and 2.5 μm they have been further rebinned to a resolution of 500 between 0.5 and 0.987 μm in order to become directly comparable to the observed spectra. Figure 2 shows the identifications of the molecular bands in the observed wavelength range. In this region, the main molecular contributors are CO, C_2 and CN.

The effects of changes in the stellar parameters are summarised in Fig. 3. The parameters the spectral features are most sensitive to are the effective temperature and the C/O ratio. A lower effective temperature leads to a shift of the maximum of the energy distribution to the red and to stronger C_2 and CN features; a higher C/O ratio results in a shift of the maximum to the blue, to stronger C_2 and CN features and to weaker CO features. $^{12}C/^{13}C$ also has a significant influence on the feature strengths. A lower $^{12}C/^{13}C$ ratio results in a shift of the maximum of the energy distribution to the blue and generally in weaker features. The effects of $\log(g)$ and of the micro-turbulent velocity $v_{\rm mic}$ are small in comparison to the temperature and C/O effects. The CO features become stronger if the star is more extended ($\log(g)$ becomes smaller), C_2 and CN features behave in the opposite way. Increasing the value of $v_{\rm mic}$ results in weaker features.

The effects of the various model parameters are not independent of each other (see also Sect. 7). For instance, as long as the $^{12}C/^{13}C$ ratio remains a free parameter

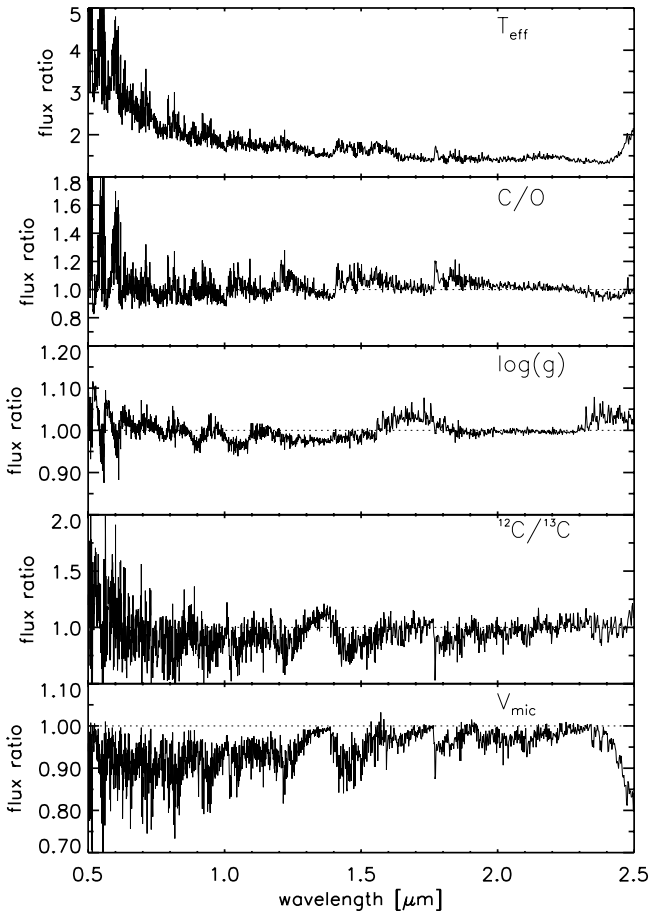

Fig. 3. From top to bottom: flux ratio of models with $T_{\rm eff} = 3200$ K and 2800 K (C/O = 1.1 in both cases, $\log(g)$ was adjusted in order that both models have the same luminosity); flux ratio of C/O = 1.1 and 1.4 for a model with $T_{\rm eff} = 3200$ K and $\log(g) = +0.0$; flux ratio of $\log(g) = +0.0$ and -0.7 for models with $T_{\rm eff} = 3200$ K and C/O = 1.1; flux ratio of $^{12}C/^{13}C = 89$ and 3.5 for a model with $T_{\rm eff} = 2800$ K and $\log(g) = -0.67$; flux ratio of $v_{\rm mic} = 3$ and 5 km s^{-1} for models with $T_{\rm eff} = 2800$ K, C/O = 1.1 and $\log(g) = -0.67$

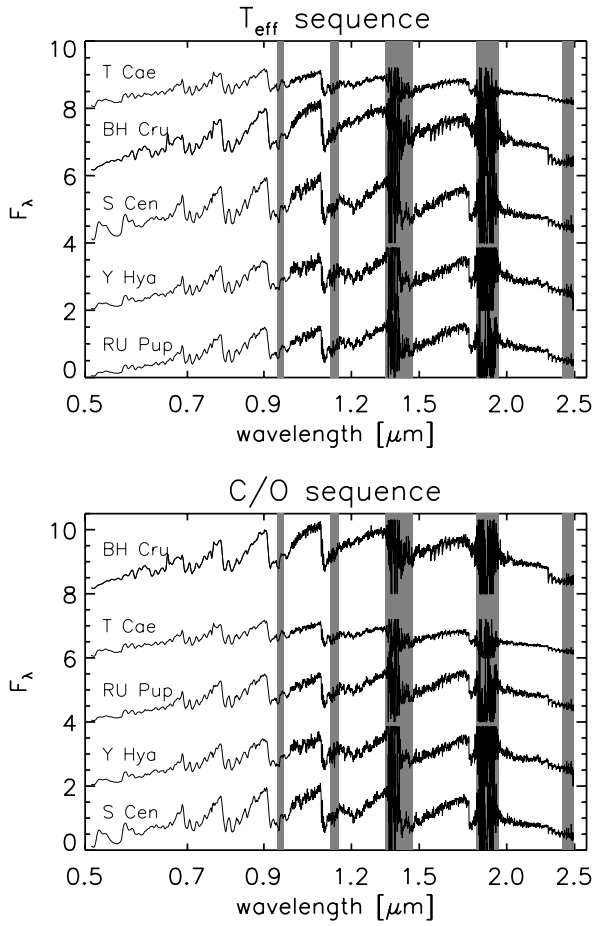

Fig. 4. Sequence of decreasing effective temperatures of our sample stars (from top to bottom in upper panel) and sequence of increasing C/O ratio (increasing from top to bottom in lower panel). The grey shaded areas mark regions of the spectra which are contaminated by the Earth's atmosphere

(because its determination is difficult at low spectral resolution) the derived effective temperatures and C/O ratios are affected by uncertainties. We calculated opacity sampling data for all included molecules with $^{12}C/^{13}C$ ratios of 89 (the solar value), 3.5 (the CNO cycle equilibrium, which is the theoretical minimum value) and 40 (an intermediate value). Varying the $^{12}C/^{13}C$ ratio between 3.5 and 89 typically results in a best fit obtained with a difference in effective temperature of 100 K and a difference in the C/O ratio of about 0.05. Therefore we want to stress that best fits as those presented in the following sections, are never necessarily unique fits.

5. Comparison of observed spectra and model spectra

Since the variations in the spectra are small, we have selected one particular spectrum of each star (the January 1996 data) for a detailed comparison with the models.

As main temperature indicators the overall energy distributions were used and especially the intensities of the CN features at 0.69, 0.78, 1.08 and around 1.46 μm. Once the temperature range was determined we tried to fix the C/O ratio. As main C/O ratio indicators we used the CO band at 2.29 and the C_2 bands at 0.77, 0.88, 1.02, 1.20 (all belonging to the Phillips system) and 1.77 μm (Ballik-Ramsay fundamental band). Unfortunately the absorption coefficient of C_2 beyond 1.1 μm is quite uncertain (see Sect. 4). Therefore the unblended 1.77 μm C_2 band is less suitable for the determination of the C/O ratio than expected. Figure 4 shows the result of an attempt to put our stars in a sequence of decreasing effective temperature (upper panel) and in a sequence of increasing C/O ratio (lower panel).

For the stars in our sample not a lot of other observational data and analyses in the literature exist. As shown by Jørgensen et al. (2000) the 3 μm C_2H_2/HCN and the 5.1 μm C_3 features are powerful tools to determine effective temperatures and C/O ratios for relatively hot carbon stars surrounded only by small amounts of dust. Unfortunately no spectra covering these two regions

simultaneously exist for our sample stars. Therefore the parameters derived for the stars are based only on our spectra covering the wavelength region between 0.5 and 2.5 μm.

6. Discussion of the individual stars

6.1. BH Cru

BH Cru had been classified as an SC star with strong ZrO and no C_2 bands, in 1965 to 1973 by Catchpole & Feast (1971) and by Keenan & Boeshaar (1980). In 1980, Lloyd Evans (1985) found moderately strong C_2 and probably no ZrO bands, in 1984 C_2 was strong and ZrO absent. Since then he had followed the star around its pulsation cycle and finds it to be a stable CS star with no ZrO bands (Lloyd Evans, private communication). Bedding et al. (2000) show that during the same time the period of the star has increased from 421 to about 535 days today, around the time of our observations the period was about 520 days. The IRAS-LRS spectrum of BH Cru is essentially continuous with a hint of circumstellar emission (Lambert et al. 1990). Therefore the star is not surrounded by a lot of dust. Kipper & Wallerstein (1990) analysed the wavelength region 6685 to 6721 Å of SC stars. They determined Li abundances and abundances of a few other elements. For this determination they adopted a model atmosphere with $T_{\rm eff} = 3500$ K, $\log(g) = 0.0$, C/O = 1.00 and $M = 2\ M_\odot$ for BH Cru. Abia & Isern (1997) derived a $^{12}C/^{13}C$ ratio of 8, assuming an effective temperature of 3500 K for the star. Abia & Wallerstein (1998) analysed spectra taken in the wavelength region between 4850 an 9300 Å with a resolution of 20 000. Their spectrum showed the H_α line in emission, the observation was made close to the visual maximum light. They determined abundances of heavy elements. For their analysis they used a model with an effective temperature of 3500 K, a $\log(g)$ of 1.0, a mass of 2 $M_\odot$ and a C/O ratio of 1.00 which they assume as representative values for SC stars.

The previous observations of BH Cru imply that the C/O ratio of BH Cru has to be close to 1.00. The effective temperatures and $\log(g)$ values used in previous studies were only representative values for SC stars (Abia & Wallerstein 1998), and we therefore put lower weight to them as measures for a specific star. Our spectrum of BH Cru taken in January 1996 was obtained close to the visual maximum (phase 0.03 according to AAVSO data). It shows the H_α line at 6565 Å in emission.

We are able to obtain a good fit (see Fig. 5) with $T_{\rm eff} = 3200$ K, $\log(g) = 0.0$, C/O = 1.01 and $v_{\rm mic} = 3\,{\rm km\,s^{-1}}$ when adopting $^{12}C/^{13}C = 3.5$ (which is the value closest to the ratio of 8 determined by Abia & Isern (1997) for which we have computed opacity sampling data). In the uppermost panel of Fig. 5 the observed spectrum of BH Cru (black line) and the model spectrum (grey line) are plotted together. In the panel below, the flux ratio of observed spectrum and the model spectrum is shown. The grey shaded areas always mark regions of the spectra which are contaminated by the Earth's atmosphere. The spectra have been forced to have equal flux at a wavelength of 1.29 μm. Below these two panels four zooms of the uppermost plot are plotted, showing the main bands which have been used for the determination of effective temperature and C/O ratio. In addition the identifications of the molecular bands are given. In the last of these four small plots, the one showing the CO 2.29 μm band, we have forced the fluxes of observed and model spectra to be equal at the CO band head at 2.29 μm, in order to make the determination of the C/O ratio easier.

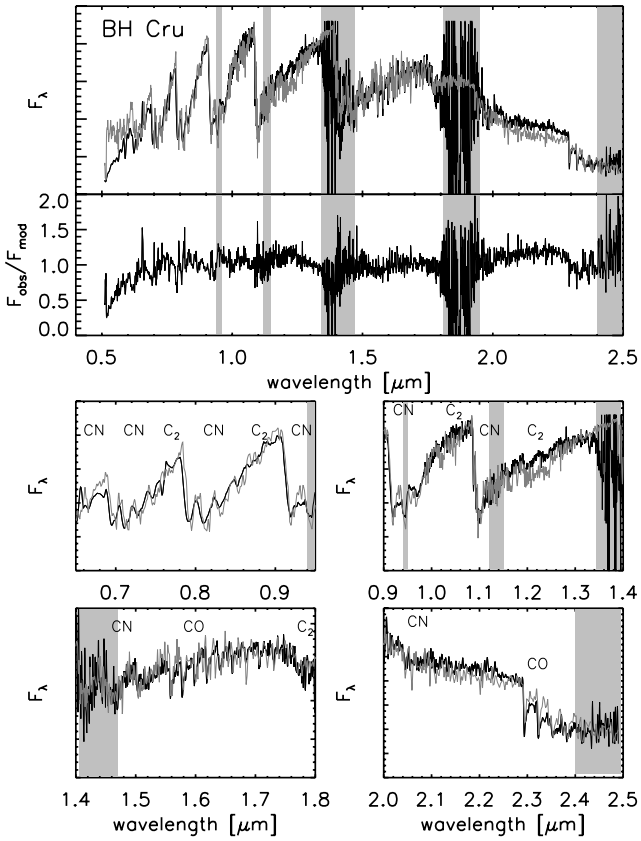

Fig. 5. In the uppermost panel the observed spectrum of BH Cru (black line) and the model spectrum (grey line) are plotted, below that the flux ratio of observed and model flux. The spectra have been forced to have equal flux at a wavelength of 1.29 μm. Below four zooms of the uppermost plot are shown and the identifications of the molecular bands are given. The parameters of the model are: $T_{\rm eff} = 3200$ K, $\log(g) = 0.0$, C/O = 1.01, $v_{\rm mic} = 3\,{\rm km\ s^{-1}}$ and $^{12}C/^{13}C = 3.5$. In the last zoom we have forced the fluxes of observed and model spectra to be equal at the CO band head at 2.29 μm

The discrepancy between observation and model from 0.5 to approximately 0.7 μm (which exists in all stars we looked at) will be discussed in detail in Sect. 6.6. The overall energy distribution and the intensities of the CN, CO and the C_2 bands at 0.77, 0.88, 1.02 and 1.77 μm fit very well, while the computed C_2 band at 1.20 μm is too strong. There is also some discrepancy obvious at 1.79 μm,

which is a common feature of all stars and will therefore be discussed in Sect. 6.6.

BH Cru is the only star in our sample showing strong variability. The spectrum closest to minimum light which we have (July 1996; phase 0.34) can be fitted with a spectrum based on a hydrostatic model with an effective temperature of 2800 K if all the other parameters used for the fit of the January 1996 spectrum are kept constant.

6.2. T Cae

T Cae is classified as a C6,4 (N4) star in the GCVS of Kholopov et al. (1988). In his revised classification for C stars Keenan (1993) assigned to T Cae the C_2 index 4.5. The star was observed twice by Baumert (1972) in the Wing filter system. From these measurements between 7117 and 10 975 Å he derived colour temperatures of 2926 and 3115 K at the date of his observations. The IRAS-LRS spectrum shows evidence of weak SiC emission at 11.3 μm.

Figure 6 shows our best fit obtained with $T_{\rm eff} = 3400$ K, $\log(g) = 0.0$, C/O = 1.05 and $v_{\rm mic} = 3\,{\rm km\,s^{-1}}$ when adopting $^{12}{\rm C}/^{13}{\rm C} = 3.5$. For T Cae no determination of the $^{12}{\rm C}/^{13}{\rm C}$ ratio exists, we chose 3.5 because the model spectrum matched the observation best in this case. It has not been determined by a detailed line analysis. A difference between our effective temperature and the colour temperatures of a few hundred degrees is as expected. Also in the case of the irregular variable carbon star TX Psc the colour temperature of Baumert was 200 to 300 K below the effective temperature determined with detailed hydrostatic model atmospheres (Jørgensen et al. 2000).

The overall energy distribution, the CN, CO and the C_2 bands at 0.77, 0.88, 1.02 and 1.20 μm fit very well, while the synthetic C_2 band at 1.77 μm is too weak. In addition to the minor general discrepancies between observation and model spectra in common for all the stars (and which will be discussed in Sect. 6.6), we remark that the observed spectrum shows a flux excess compared to the model beyond about 1.7 μm. This could be caused either by a contribution of warm dust around the star or by dynamic effects which we are not accounting for in our hydrostatic models. The star has only a very weak 11.3 μm SiC feature, hinting that the amount of dust around the star could be small.

6.3. S Cen

S Cen is classified as a C star in the GCVS of Kholopov et al. (1988). Chan (1994) calls S Cen a "stellar blackbody source" based on its IRAS-LRS data. There is no sign of a SiC emission feature, only an excess in the 60 and 100 μm flux, hence there is no sign of warm dust around this star. The star was observed twice by Baumert (1972) in the Wing filter system. From these measurements he derived colour temperatures of 2928 and 2909 K at the date of his observations.

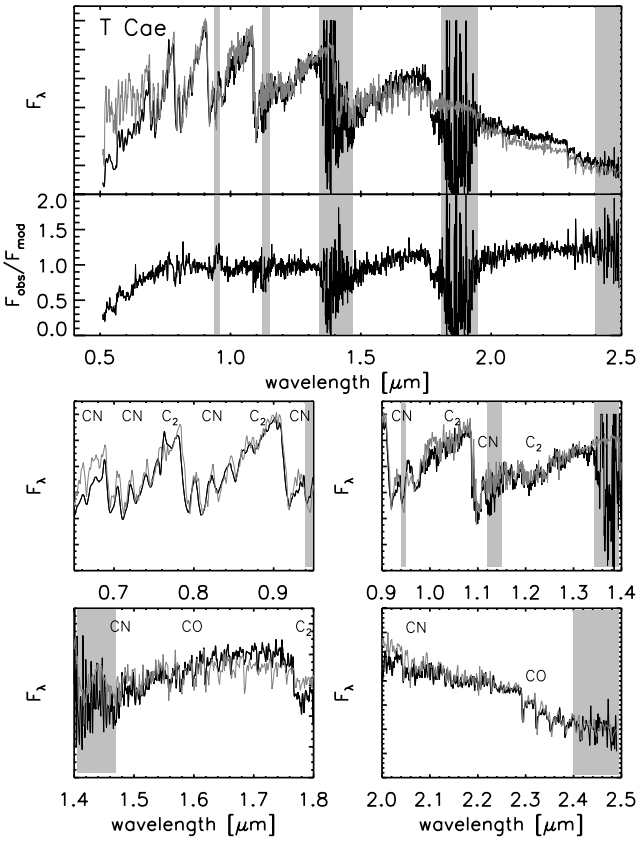

Fig. 6. Best fit to the spectrum of T Cae. The plot layout is the same as in Fig. 5. The parameters of the model are: $T_{\rm eff} = 3400$ K, $\log(g) = 0.0$, C/O = 1.05, $v_{\rm mic} = 3\,{\rm km\,s^{-1}}$ and $^{12}{\rm C}/^{13}{\rm C} = 3.5$

Figure 7 shows our best fit obtained with $T_{\rm eff} = 3100$ K, $\log(g) = 0.0$, C/O = 1.4 and $v_{\rm mic} = 3\,{\rm km\,s^{-1}}$ when adopting $^{12}{\rm C}/^{13}{\rm C} = 40$. For S Cen, where no determination of the $^{12}{\rm C}/^{13}{\rm C}$ ratio exists, we chose 40 because the model spectrum matched the observation best in this case. It has not been determined by a detailed line analysis.

The overall energy distribution and the intensities of the CN bands, the CO bands and the C_2 bands at 0.77 and 1.77 μm fit very well, while the computed C_2 bands at 0.88 and 1.02 μm are stronger than observed.

6.4. RU Pup

RU Pup is classified as a C5,4 star in the GCVS of Kholopov et al. (1988). In his revised classification for C stars Keenan (1993) assigned to RU Pup the C_2 index 7. Claussen et al. (1987) looked at a sample of Galactic carbon stars taken from the *Two Micron Sky Survey* to provide estimates of their space distribution and mass-loss rates. For RU Pup they derived a distance of 1.03 kpc, a mass-loss rate of $10^{-6.8}\,M_\odot$/yr and a luminosity of $7300\,L_\odot$. The IRAS-LRS spectrum shows weak SiC emission at 11.3 μm. The star was observed four times by Baumert (1972) in the Wing filter system. From these measurements he derived colour temperatures between 2760 and 2785 K at the dates of his observations.

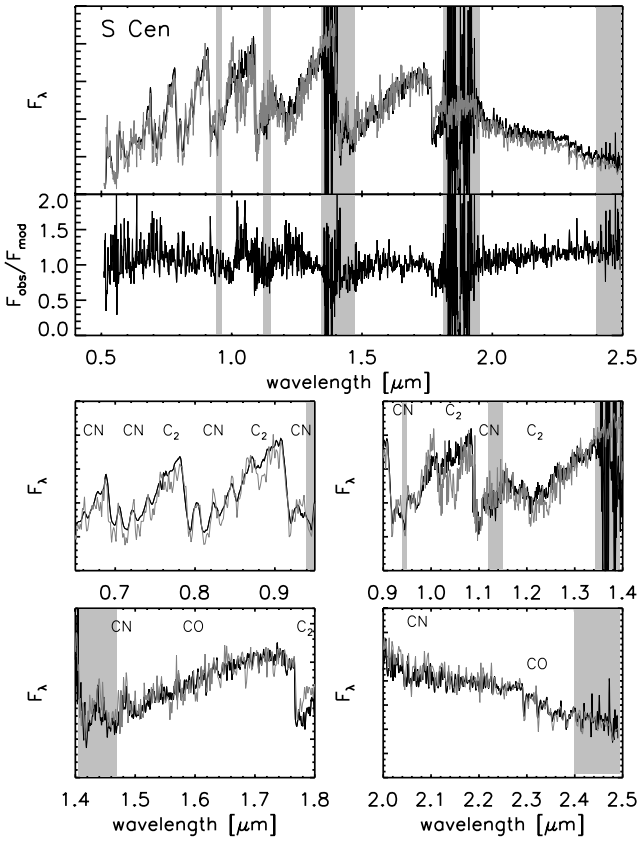

Fig. 7. Best fit to the spectrum of S Cen. The plot layout is the same as in Fig. 5. The parameters of the model are: $T_{\rm eff} = 3100\,{\rm K}$, $\log(g) = 0.0$, ${\rm C/O} = 1.40$, $v_{\rm mic} = 3\,{\rm km\,s^{-1}}$ and $^{12}{\rm C}/^{13}{\rm C} = 40$

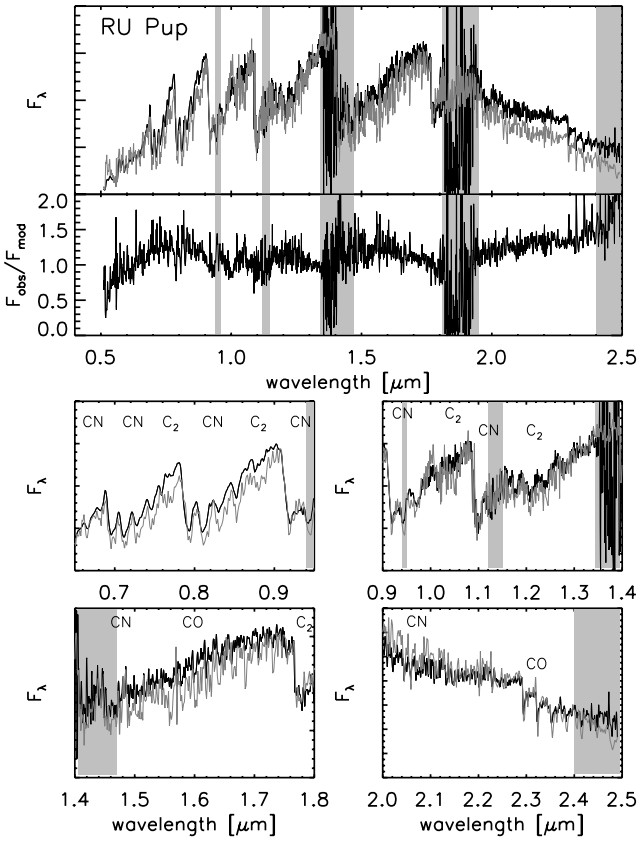

Fig. 8. Best fit to the spectrum of RU Pup. The plot layout is the same as in Fig. 5. The parameters of the model are: $T_{\rm eff} = 2900\,{\rm K}$, $\log(g) = -0.61$, ${\rm C/O} = 1.10$, $v_{\rm mic} = 3\,{\rm km\,s^{-1}}$ and $^{12}{\rm C}/^{13}{\rm C} = 89$

S. Bagnulo (private communication) provided us with unpublished photometry from B to L from March 1997 at SAAO which is about one cycle later than our own observation of January 1996. A blackbody fit to the photometry resulted in a blackbody temperature of 2260 K and a dust temperature of 400 K (see Kerschbaum & Hron 1996 for details of the fitting). We obtain the best fit of our spectrum with an effective temperature of 2900 K. This is in good agreement with the finding of Kerschbaum & Hron (1996) that the effective temperature of semi-regular variables is usually about 500 K higher than the blackbody temperature. Tanaka et al. (1996) measured infrared indices of RU Pup two times. One of their observations was done close to ours, also in January 1996. Their colour index, which they suggest as a good measure of the effective temperature, gives support to an effective temperature of the star of 2900 K at that time.

Figure 8 shows our best fit obtained with $T_{\rm eff} = 2900\,{\rm K}$, $\log(g) = -0.61$, ${\rm C/O} = 1.1$ and $v_{\rm mic} = 3\,{\rm km\,s^{-1}}$ when adopting $^{12}{\rm C}/^{13}{\rm C} = 89$. For RU Pup no determination of the $^{12}{\rm C}/^{13}{\rm C}$ ratio exists, we chose 89 because the model spectrum matched the observation best in this case. It has not been determined by a detailed line analysis. The $\log(g)$ value of -0.61 was chosen in order to match the derived luminosity of Claussen et al. (1987).

The overall energy distribution and the intensities of the CN bands and the C_2 band at 1.77 μm fit well, while the CO bands and the C_2 bands at 0.77, 0.88, 1.02 and 1.20 μm are too strong. This suggests that the adopted C/O ratio of RU Pup is slightly too high. As for T Cae, we remark that the observed spectrum shows a flux excess compared to the model beyond about 1.7 μm, which could be caused either by a contribution of warm dust around the star or by dynamic effects which we are not accounting for in our hydrostatic models. The presence of the SiC feature indeed suggests the existence of circumstellar dust. However, if its blackbody temperature is 400 K as indicated by the photometry, the contribution of the dust to the 2 μm flux should be small.

6.5. Y Hya

Y Hya is classified as a C5,4 (N3F) star in the GCVS of Kholopov et al. (1988). Claussen et al. (1987) derived a distance of 0.54 kpc and a luminosity of $5500\,L_\odot$ for Y Hya. Lambert et al. (1986) determined a C/O ratio of 1.52 and a $^{12}{\rm C}/^{13}{\rm C}$ ratio of 82 for this star, when an effective temperature of 2770 K was adopted. In contrast to that, Ohnaka & Tsuji (1996) have determined a $^{12}{\rm C}/^{13}{\rm C}$ ratio of 25 for Y Hya, based on an effective temperature determined with the infrared flux method of

3050 K. Eglitis & Eglite (1995) derive a C/O ratio of 1.46. S. Bagnulo (private communication) provided us with unpublished photometry from March 1997 at SAAO, but the data were not sufficient to determine a very reliable blackbody temperature. However, we can see that Y Hya must have a higher effective temperature than RU Pup, so the photometric data do not support the low effective temperature value adopted by Lambert et al. (1986). Tanaka et al. (1996) measured infrared indices of Y Hya three times. Their observations were done 8, 4 and 3 years before our own observation in January 1996, respectively. Their colour index, which they suggest as a good measure of the effective temperature, gives support to effective temperatures of the star of 3100, 2600 and 2800 K at the time of their observations. This might indicate that Y Hya can vary remarkably, but it did not during the time we observed it. We found indication of similar sudden, irregular variation in the effective temperature of TX Psc in our recent ISO study of three carbon stars (Jørgensen et al. 2000).

Figure 9 shows our best fit obtained with $T_{\rm eff} = 3100$ K, $\log(g) = -0.40$, C/O = 1.4 and $v_{\rm mic} = 3\,{\rm km\,s^{-1}}$ when adopting $^{12}{\rm C}/^{13}{\rm C} = 89$. For Y Hya two determinations of the $^{12}{\rm C}/^{13}{\rm C}$ ratio exist and they give remarkably different results. Lambert et al. (1986) derived a value of 82 from the CN $\Delta v = -2$ sequence around 2 μm, while Ohnaka & Tsuji (1996) determined a value of 25 using lines of the CN red system around 8000 Å, based on the iso-intensity method and line-blanketed model atmospheres. We therefore tried to find best fits for $^{12}{\rm C}/^{13}{\rm C}$ ratios of 40 and 89. We obtained a better fit with a $^{12}{\rm C}/^{13}{\rm C}$ ratio of 89. The $\log(g)$ value of -0.40 was chosen in order to match the derived luminosity of Claussen et al. (1987).

The overall energy distribution and the intensities of the CN bands and the C_2 bands at 0.77, 0.88 and 1.77 μm fit well, while the computed CO bands and the C_2 bands at 1.02 and 1.20 μm are stronger than observed. As for T Cae and RU Pup, the observed spectrum shows a flux excess compared to the model beyond about 1.7 μm, with the same potential reasons.

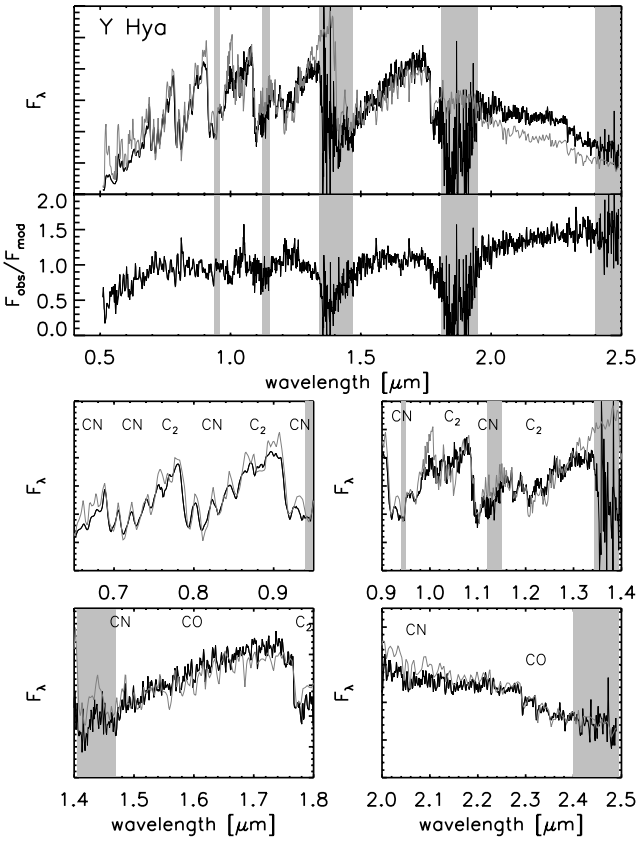

Fig. 9. Best fit to the spectrum of Y Hya. The plot layout is the same as in Fig. 5. The parameters of the model are: $T_{\rm eff} = 3100$ K, $\log(g) = -0.40$, C/O = 1.40, $v_{\rm mic} = 3\,{\rm km\,s^{-1}}$ and $^{12}{\rm C}/^{13}{\rm C} = 89$

6.6. Discussion

From our fits of the spectra we obtained a sequence of effective temperatures and C/O ratios of our sample stars (see Fig. 4). We derived an increasing C/O sequence from BH Cru, T Cae, RU Pup, Y Hya to S Cen. From its classification and the reports in the literature about the ongoing transition from a SC to a C star it was clear that BH Cru will be the star with the lowest C/O ratio in our sample. Support for the lower C/O ratio of T Cae compared to RU Pup comes from the revised classification for C stars of Keenan (1993) who assigned T Cae a smaller C_2 index (4.5) than RU Pup (7). Y Hya was already mentioned in the literature as a star with high C/O ratio. For the effective temperatures, we found a decreasing sequence from T Cae, BH Cru/S Cen, Y Hya to RU Pup for the time of our observations in January 1996. However, especially BH Cru (which is a Mira) can vary its effective temperature during the cycle, and although we estimate the effective temperature to have been 3200 K in January 1996, the other two spectra obtained at about phase 0.26 and 0.34 can be nicely fitted with effective temperatures of about 2800 K, ranking BH Cru cooler than RU Pup, the coolest star in our January 1996 sample. The other stars in our sample did not change much during the period we observed them. But in the case of Y Hya there is evidence from other measurements (see Sect. 6.5) for changes in effective temperature which probably do not occur regularly. While our own determination of the effective temperature resembles close the one of Ohnaka & Tsuji (1996), the measurement of Tanaka et al. (1996) taken in 1988 and photometry provided by S. Bagnulo from 1997, two other measurements of Tanaka et al. (1996) taken in 1992 and 1993 support the determination of Lambert et al. (1986).

In the fit of the spectra there are some systematic discrepancies. The most obvious discrepancy is that the models have much more flux in the wavelength range between 0.5 and approximately 0.7 μm than the observed spectra. We do not include atomic lines in our spectrum calculation. The discrepancy is larger the hotter the model and the lower the C/O ratio. While the fit of S Cen is quite good in the whole range (high C/O ratio, "modest" $T_{\rm eff}$),

the one of T Cae is bad shortwards of 0.7 μm (low C/O ratio, "high" $T_{\rm eff}$). This hints on the fact that these discrepancies are mainly due to the lack of the inclusion of the atomic lines in our calculations.

The second discrepancy is the "flux excess" of the observations longwards of approximately 1.7 μm compared to the models which is very pronounced in RU Pup and especially Y Hya, and small, but still present, in BH Cru, T Cae and S Cen. The discrepancy seems to become worse the cooler the star and the higher the C/O and ^{12}C/^{13}C ratio. We think that the reason for this disagreement is either due to the contribution of dust surrounding the star or to dynamic effects which we can not account for in hydrostatic models.

The third discrepancy occuring in all spectra is at 1.78 to 1.79 μm. In our synthetic spectra this wavelength region is dominated by the fundamental C_2 Ballik-Ramsay band. The bandhead at 1.77 μm can be fitted, but the region beyond not. In all observed spectra the feature at 1.78 μm is stronger than the C_2 bandhead. We are lacking some opacity at this wavelength.

There is also some discrepancy visible longwards of about 2.40 μm in all spectra, but this is due to noise (and therefore this region was superposed by a shaded area too).

7. Fundamental stellar parameters and spectrophotometric indices

Obtaining simultaneous spectra over the whole optical and near-IR spectral range is not practical. Spectrophotometric indices can be obtained and reduced much more rapidly. It is therefore desirable to find indices to estimate the fundamental stellar parameters, and to provide the corresponding calibrations.

With this purpose in mind, we have measured a large number of indices both on the empirical carbon star spectra and on 132 available models (see Sect. 4). The indices included 65 possible combinations of filters chosen inside the commonly used sets of:
(i) *VRIJHK* broad band filters as defined in Bessell (1990), except that the V and K band have been truncated at 5100 and 24 500 Å respectively, to match the wavelength range available in the data;
(ii) intermediate filters that we call "Wing filters" for brevity, which were initially defined by Wing (1967) and are summarised by Bessell et al. (1989);
(iii) Hubble Space Telescope NICMOS filters, which were obtained from the Space Telescope Science Institute (1997). The narrow filter transmissions were modelled as rectangles with appropriate central wavelengths and bandwidths, $F108$ (see Table 3) is on Camera 1, all others are on Camera 2;
(iv) two fine CO measurements. The index measuring the equivalent width of the CO 2-0 bandhead at 2.29 μm as explained by Kleinmann & Hall (1986) we call CO1. The second index, COH, measures the ratio of the flux density between 16 182 and 16 262 Å to the average of the flux densities in two narrow windows on either side of the CO feature; one between 16 145 and 16 175 Å, the other between 16 270 and 16 300 Å.

Table 3. Filter names, positions and widths

name	central wavelength [μm]	filter width [μm]
V	0.545	0.230
R	0.600	0.350
I	0.805	0.220
J	1.220	0.300
H	1.630	0.380
K	2.190	0.540
$W710$	0.710	0.006
$W883$	0.883	0.0045
$W888$	0.888	0.0045
$W110$	1.100	0.006
$W123$	1.236	0.012
$F108$	1.083	0.0108
$F110$	1.100	0.06
$F171$	1.715	0.07
$F180$	1.800	0.07
$F222$	2.150	0.15

Using the whole set of model spectra, the linear correlation coefficient and Spearman's rank correlation coefficient were computed between each index and, respectively, effective temperature, the ^{12}C/^{13}C ratio, the C/O ratio and surface gravity $\log(g)$. This led to a first selection of potentially useful indices. The indices are magnitude differences plus a constant chosen to ensure that all indices take a value of zero for a Vega model. Table 3 summarises the names and properties of the filters which turned out to be useful in our investigations.

7.1. Effective temperature indicators

The range of temperatures relevant for carbon-rich AGB stars is large, and the effect of this parameter on the energy distribution is strong. In the sample of theoretical spectra, linear correlation coefficients larger than 0.975 (absolute value) were obtained between $T_{\rm eff}$ and $V-K$, $R-K$, $R-H$, $R-J$, $W710-W123$ (and colour indices combining filters from two different filter subsets). The correlations obtained with $R-J$, $R-H$ and $W710-W123$ are the strongest. This is fortunate, since the filters used there are still located in relatively central parts of the spectra, where the agreement between the energy distributions of the models and the data is good. The correlations are shown in Figs. 10–12. In similar plots for colours including V or K band measurements, there is a stronger *systematic* shift between the loci of the data and the models. This shift is due to the already mentioned "flux excess" of

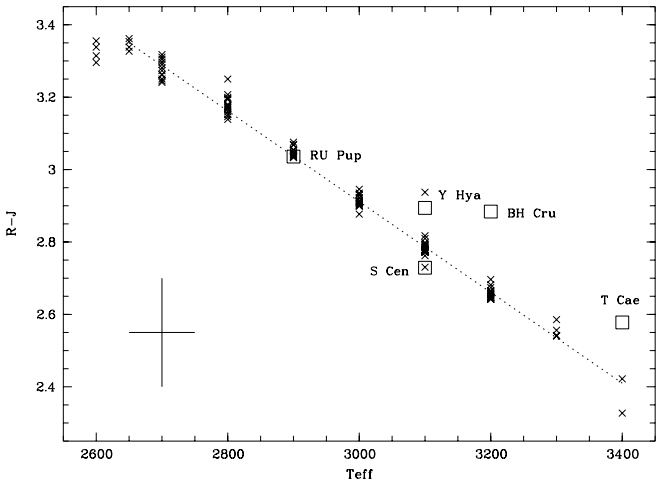

Fig. 10. $R-J$ as an effective temperature indicator for carbon rich stars. Each cross represents a model spectrum. The dashed line shows the linear least squares regression: $T_{\rm eff}\,(K) = 5320 - 797\,(R-J)$. The squares represent the January 1996 spectra; they are located at the effective temperature resulting from the adjustment of the whole wavelength range, for which not only broad band colours but also spectral features play a role. The vertical bar indicates the $2\,\sigma$ uncertainty on the colours of the data points. The horizontal bar accounts for the range of effective temperatures allowed with equally satisfactory fits

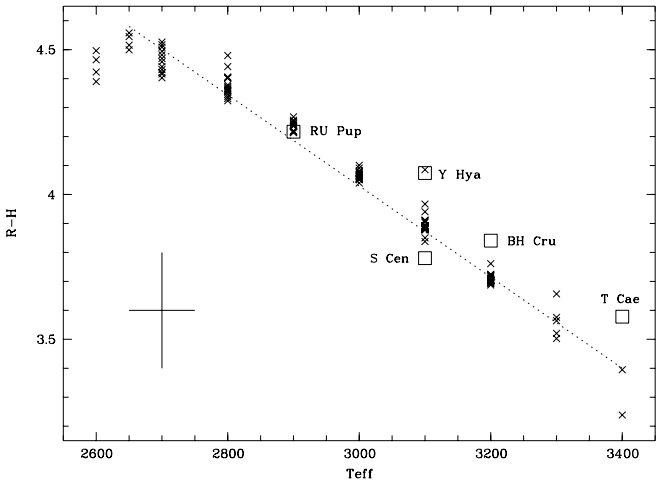

Fig. 11. $R-H$ as an effective temperature indicator. The linear regression line writes: $T_{\rm eff}\,({\rm K}) = 5585-640\,(R-H)$

the observations compared to the models in the K filter and the lack of the inclusion of atomic lines in our models in the V filter.

7.2. $^{12}C/^{13}C$ indicators

In the sample of model spectra, the spread around the mean relations between $T_{\rm eff}$ and the temperature sensitive colours is too small to be useful in constraining other stellar parameters. Other indices have to be selected. Since models exist for only three values of the $^{12}{\rm C}/^{13}{\rm C}$ ratio, Spearman's rank correlation coefficient is not a selective

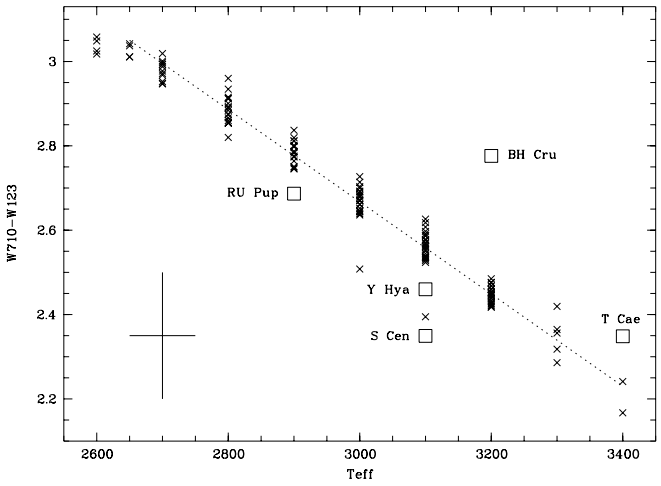

Fig. 12. The intermediate band colour index $W710-W123$ as a $T_{\rm eff}$ indicator. The linear regression line writes: $T_{\rm eff}\,({\rm K}) = 5445 - 33\,(W710-W123)$

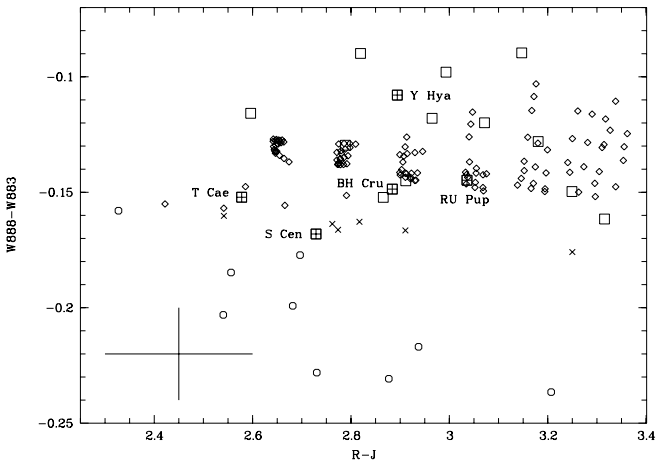

Fig. 13. The $^{12}{\rm C}/^{13}{\rm C}$ indicator $W888-W883$ versus $T_{\rm eff}$, as measured by $R-J$. Small symbols are models, computed respectively with $^{12}{\rm C}/^{13}{\rm C} =$ 89 (lozenges), 40 (crosses) and 3.5 (circles). Large squares are measurements on empirical data; crossed squares locate the January 1996 data, for which a spectral fit has been performed. $2\,\sigma$ uncertainties on the empirical data are shown

tool to pick up useful indicators; it hasn't been used. The tightest linear correlation with $^{12}{\rm C}/^{13}{\rm C}$ was obtained for $W888-W883$ (correlation coefficient = 0.84). The two colour plot obtained by combining this index with, for instance, $R-J$ in principle simultaneously allows us to determine $T_{\rm eff}$ and to constrain the value of $^{12}{\rm C}/^{13}{\rm C}$.

Figure 13 shows that the locus of the models and the data agree relatively well in the two colour diagram. Most of the data indicate high values of the $^{12}{\rm C}/^{13}{\rm C}$ ratio. In particular, this is the case for Y Hya, in agreement with the spectral fit. The four highest observed values of the $W888-W883$ belong to this star. In view of the observational uncertainties, it is not surprising that the $^{12}{\rm C}/^{13}{\rm C}$ values that came out of the spectral fit are not always equal to the values suggested by $W888-W883$ for the other objects.

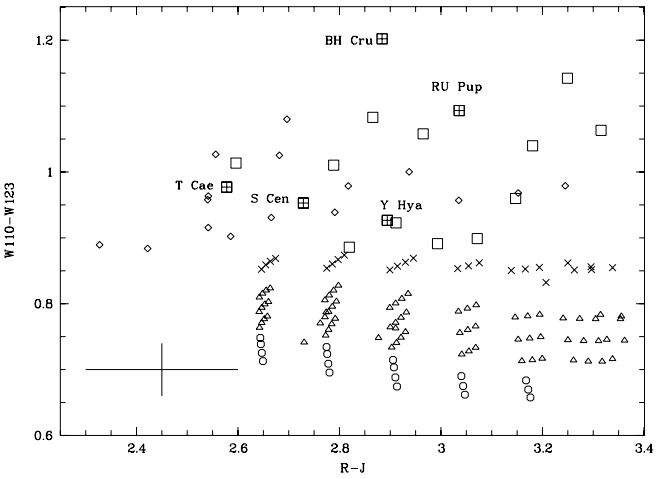

Fig. 14. The C/O indicator $W110-W123$ versus $T_{\rm eff}$, as measured by $R-J$. Small symbols are models, computed respectively with $\mathrm{C/O} < 1.1$ (lozenges), $1.1 \leq \mathrm{C/O} \leq 1.2$ (crosses), $1.2 < \mathrm{C/O} \leq 1.4$ (triangles) and $1.4 < \mathrm{C/O} \leq 1.8$ (circles). Large squares are measurements on empirical data; crossed squares locate the January 1996 data, for which a spectral fit has been performed. $2\,\sigma$ uncertainties on the empirical data are shown

7.3. C/O indicators

The best linear and rank correlations with the C/O ratio is obtained for the intermediate band colour index $W110-W123$ (linear correlation coefficient $= -0.853$, rank correlation $= -0.938$). Other potentially useful indices include the HST/NICMOS colours $F180-F171$, $F180-F222$ and $F108-F110$, and, rather surprisingly, the equivalent widths of the CO bandheads measured by COH and CO1.

The two colour plot of Fig. 14 in principle allows us to simultaneously determine the effective temperature and estimate the C/O ratio. Although there seems to be a systematic offset between the loci of the empirical and the model indices in the sense that empirical values of $W110-W123$ are larger by about 0.1 magnitude than those of the models, there is a large region of overlap. In addition, the ranking of the observed stars on a C/O sequence obtained from the $W110-W123$ index is identical to the ranking obtained from the adjustment of the whole spectrum, with the exception of T Cae (based on the colour index, this would be given a larger C/O value than RU Pup). The 7 data points with the lowest $W110-W123$ indices correspond to Y Hya and S Cen, the two stars with the highest previously estimated C/O values.

7.4. Surface gravity indicators

The effects of gravity over the range of parameters explored in this paper are small compared to those of C/O or $^{12}\mathrm{C}/^{13}\mathrm{C}$. As already mentioned, the reason for the low sensitivity of the near-IR spectral range to surface gravity lies in the relatively high temperatures (i.e. deep stellar layers) at which the main relevant molecules form. No spectrophotometric index was found capable of providing useful direct constraints on $\log(g)$.

Table 4. Results of our fits

name	$T_{\rm eff}$ [K]	$\log(g)$	C/O	$^{12}\mathrm{C}/^{13}\mathrm{C}$	$\Delta T_{\rm eff}$ [K]
BH Cru	3200	0.00	1.01	3.5	≈400
T Cae	3400	0.00	1.05	3.5	≈200
S Cen	3100	0.00	1.40	40	≈100
RU Pup	2900	−0.61	1.10	89	≈100
Y Hya	3100	−0.40	1.40	89	≈200

7.5. Discussion

$T_{\rm eff}$, $^{12}\mathrm{C}/^{13}\mathrm{C}$ and C/O can in principle be determined from broad and intermediate band colour indices such as those identified here. We have been able to find indices for which no or small *systematic* differences exist between the loci of measurements on models and on data. In the case of C/O, a correction of the suggested $W110-W123$ index of 0.1 magnitude provides quantitative agreement with the models. Very good photometry is needed to actually use these diagnostic plots.

A full multivariate analysis can be performed to determine the combinations of the fundamental stellar parameters that can be best determined with the empirical indices. In view of the currently remaining systematic differences between the models and quite a few of the indices, we postpone this to future times.

8. Conclusions

For the first time we were able to fit spectra of carbon stars in the huge wavelength region all the way from 0.5 to 2.5 μm, based on spectra taken simultaneously and therefore at the same pulsational phase. On the observational side this became possible due to the unique possibility of taking spectra of the stars simultaneousily in several spectral regions. On the theoretical side this is mainly due to the drastic improvement of available molecular opacitites. The stars chosen for the comparison with spectra based on hydrostatic model atmospheres are (with one exception – BH Cru, which is a Mira star) so called semi-regular variables which vary only moderately during their pulsational cycle. We restricted ourselves to analyse in detail only the spectra taken in January 1996, because it is not possible to model the variations in the spectra self consistently with hydrostatic models.

Table 4 summarizes the results of our fits to the spectra of January 1996, giving the effective temperature, $\log(g)$, C/O ratio, $^{12}\mathrm{C}/^{13}\mathrm{C}$ ratio and in addition the changes in effective temperature that were needed to get also good fits for the spectra of the stars taken at other phases (if all other parameters than $T_{\rm eff}$ are kept constant).

Our determinations of the fundamental parameters are in good agreement with results from other methods, in the cases where such analyses exist in the literature. In the case of Y Hya there is evidence from some other measurements for changes in effective temperature which probably do not occur regularly.

A major advantage in the analysis of low resolution spectra over a wide spectral range, as presented here, is that all the fundamental parameters can be determined simultaneously. In studies of high resolution spectra it will often be necessary to adopt photometric determinations of $T_{\rm eff}$ that are not necessarily determined at the same pulsation phase as the spectrum. No general high-resolution method is known for determining $\log(g)$ in cool giant stars. The value of $^{12}C/^{13}C$ can be determined with better accuracy from high-resolution spectra, while we believe that the accuracy in the C/O determination is of the same reliability in the two methods. An additional advantage of the low-resolution method is that it can be applied to stars in remote galaxies. However, the major goal of the present paper has not been a determination of fundamental parameters, but rather a detailed test of the reliability of our model atmospheres with implications for modelling the physical structure of the upper layers of cool carbon stars, and hence for example for understanding the chemical enrichment of the Galaxy.

Our analysis has shown that the state-of-the-art of carbon star observations and modelling now, for the first time, has reached a level where a complete and self-consistent agreement between observational and computed low-resolution spectra is possible through basically all the photospheric spectral region. Combined with our previous analysis of ISO spectra (Jørgensen et al. 2000) of similar carbon stars, by use of the same models as presented here, we conclude that the agreement between synthetic and observed spectra is good for the full wavelength region from at least 5000 Å to 10 μm, and that all major spectral features can be accounted for.

Acknowledgements. We thank S. Bagnulo for providing unpublished photometry data for RU Pup and Y Hya. Discussions concerning BH Cru with T. Lloyd Evans are greatly acknowledged. We thank the referee, Dr. Tsuji, for a careful reading of the manuscript and valuable suggestions. This work made use of the Simbad and Vizier literature search tools, operated at CDS, Strasbourg. This work is supported by the Austrian Academy of Sciences (RL acknowledges an APART DOC grant), the Austrian Science Fund (FWF project S7308-AST) and by the Danish Natural Science Research Council.

References

Abia, C., & Isern, J. 1997, MNRAS, 289, L11
Abia, C., & Wallerstein, G. 1998, MNRAS, 293, 89
Alvarez, R., & Plez, B. 1998, A&A, 330, 1109
Baumert, J. H. 1972, Ph.D. Thesis at Ohio State University
Bedding, T. R., Conn, B. C., & Zijlstra, A. A. 2000, in The Impact of Large-Scale Surveys on Pulsating Star Research, ed. L. Szabados, & D. Kurtz, ASP Conf. Ser., 203, 96
Bessell, M. S. 1990, PASP, 102, 1181
Bessell, M. S., Brett, J. M., Scholz, M., & Wood, P. R. 1989, A&AS, 77, 1
Bessell, M. S., Castelli, F., & Plez, B. 1998, A&A, 333, 231
Brault, J. W., Delbouille, L., Grevesse, N., et al. 1982, A&A, 108, 201
Catchpole, R. M., & Feast, M. W. 1971, MNRAS, 154, 197
Chan, S. J. 1994, MNRAS, 268, 113
Claussen, M. J., Kleinmann, S. G., Joyce, R. R., & Jura, M. 1987, ApJS, 65, 385
Eglitis, I., & Eglite, M. 1995, Ap&SS, 229, 63
Goebel, J. H., Bregman, J. D., Goorvitch, D., et al. 1980, ApJ, 235, 104
Goorvitch, D. 1990, ApJS, 74, 769
Goorvitch, D., & Chackerian, C. Jr. 1994, ApJS, 91, 483
Gustafsson, B., Bell, R. A., Eriksson, K., & Nordlund, Å. 1975, A&A, 42, 407
Irwin, A. W. 1981, ApJS, 45, 621
Helling, C., Jørgensen, U. G., Plez, B., & Johnson, H. R. 1996, A&A, 315, 194
Höfner, S., Jørgensen, U. G., Loidl, R., & Aringer, B. 1998, A&A, 340, 497
Jørgensen, U. G. 1989, ApJ, 344, 901
Jørgensen, U. G. 1997, in Molecules in Astrophysics: Probes and Processes, ed. E. F. van Dishoek, Proc. IAU Symp., 178 (Kluwer), 441
Jørgensen, U. G., Hron, J., & Loidl, R. 2000, A&A, 356, 253
Jørgensen, U. G., Johnson, H. R., & Nordlund, Å. 1992, A&A, 261, 263
Jørgensen, U. G., & Larsson, M. 1990, A&A, 238, 424
Jørgensen, U. G., Larsson, M., Iwamae, A., & Yu, B. 1996, A&A, 315, 204
Keenan, P. C. 1993, PASP, 105, 905
Keenan, P. C., & Boeshaar, P. 1980, ApJS, 43, 379
Kerschbaum, F., & Hron, J. 1996, A&A, 308, 489
Kholopov, P. N., Samus', N. N., Frolov, M. S., et al. 1988, General Catalogue of Variable Stars, 4th Edition (Nauka Publ. House, Moscow)
Kipper, T., & Wallerstein, G. 1990, PASP, 102, 574
Kleinmann, S. G., & Hall, D. N. B. 1986, ApJS, 62, 501
Kurucz, R. F. 1994, in Molecules in the Stellar Environment, ed. U. G. Jørgensen (Springer LNP), 428, 282
Lambert, D. L., Gustafsson, B., Eriksson, K., & Hinkle, K. H. 1986, ApJS, 62, 373
Lambert, D. L., Hinkle, K. H., & Smith, V. V. 1990, AJ, 99, 1612
Lançon, A., & Wood, P. 2000, A&AS, 146, 217
Leggett, S. K., Allard, F., Dahn, C., et al. 2000, ApJ, 535, 965
Lloyd, Evans, T. 1985, in Cool stars with Excess of Heavy Elements, ed. M. Jaschek, & P.C. Keenan (Reidel), 163
Mattei, J. A. 1999, Observations from the AAVSO International Database, private communication
Ohnaka, K., & Tsuji, T. 1996, A&A, 310, 933
Querci, F., Querci, M., & Kunde, V. G. 1971, A&A, 15, 256
Querci, F., Querci, M., & Tsuji, T. 1974, A&A, 31, 265
Schultheis, M. 1998, Ph.D. Thesis at the University of Vienna
Tanaka, W., Okada, T., Hashimoto, O., et al. 1996, PNAOJ, 4, 135
Tsuji, T. 1973, A&A, 23, 411
Tsuji, T., Ohnaka, K., & Aoki, W. 1997, Proc. of Diffuse Infrared Radiation and the IRTS, ed. H. Okuda, T. Matsumoto, & T. Roellig, ASP Conf. Ser., 124
Wing, R. F. 1967, Ph.D. Thesis at the University of California (Berkeley)